

# Astigmatism correction in x-ray scanning photoemission microscope with use of elliptical zone plate

H. Ade and C.-H. Ko

*Department of Physics, State University of New York at Stony Brook, Stony Brook, New York 11794*

E. Anderson

*Center for x-ray Optics, Lawrence Berkeley Laboratory, Berkeley, California 94720*

(Received 8 August 1991; accepted for publication 11 December 1991)

We report the impact of an elliptical, high resolution zone plate on the performance of an initially astigmatic soft x-ray scanning photoemission microscope. A zone plate with carefully calibrated eccentricity has been used to eliminate astigmatism arising from transport optics, and an improvement of about a factor of 3 in spatial resolution was achieved. The resolution is still dominated by the source size and chromatic aberrations rather than by diffraction and coma, and a further gain of about a factor of 2 in resolution is possible. Sub 100 nm photoemission microscopy with primary photoelectrons is now within reach.

During the past 10–15 yr zone plates have been extensively used as high resolution optical elements in the soft x-ray region for both imaging and microprobe instruments.<sup>1</sup> Errors in the electron beam fabrication process<sup>2</sup> can result in zone plates which have elliptical rather than circular zones, introducing aberrations such as coma and astigmatism. Although this can be partially compensated for by tilting the zone plate,<sup>3</sup> great effort is generally made to produce zones as close to circular as possible<sup>4,5</sup> to minimize aberrations. Some of these quality assurance efforts, such as moire pattern techniques as described in Ref. 3, are, however, undertaken after the zone plates have been produced. Only recently did improvements in calibration standards provide enough control to assure that zone plates are circular or have a controlled and well-oriented ellipticity.<sup>6</sup> In this letter, we will demonstrate the impact of a carefully fabricated elliptical zone plate on the performance of an initially astigmatic scanning photoemission microscope.

Our instrument, the Scanning Photoemission Microscope at the soft x-ray Undulator beamline X1A (X1-SPEM) at the National Synchrotron Light Source recently recorded the first submicron images with primary photoelectrons.<sup>7,8</sup> A zone plate is used to produce a microprobe by demagnifying real images of the undulator. However, the present monochromator and x-ray transport optics places the vertical and horizontal images of the undulator for final demagnification at vastly different distances from the zone plate (2.87 m in the horizontal, versus 0.33 m in the vertical). With a 140  $\mu\text{m}$  diameter, 60 nm outermost zone width round zone plate and the use of  $\lambda = 1.86$  nm, this results in a separation of the demagnified images of 64  $\mu\text{m}$ . Since the depth of focus is only about 12  $\mu\text{m}$ , noticeable astigmatism is present. To correct for it, a well-aligned astigmatic lens with a relative focal length difference  $\Delta f/f = 1.2\%$  is needed. Since  $r_n^2 = n\lambda f$ , where  $r_n$  is the radius of the  $n$ th zone,  $\lambda$  the photon wavelength, and  $f$  the zone plate focal length, an elliptical zone plate with different focal lengths in orthogonal directions can be readily constructed by scaling the zone radii in one direction by  $1 + \epsilon$ . For our purposes,  $\epsilon = 0.006$ .

In order to assess the imaging properties of both the original uncorrected (round zone plate) and corrected configuration (elliptical zone plate) we imaged a starlike test pattern as shown in Fig. 1. It consists of 32, 100-nm-thick gold spokes plated on a 120-nm-thick  $\text{Si}_3\text{N}_4$  membrane, and has thus structure with continuously varying spatial frequencies. It allows us to measure the contrast with which these spatial frequencies and various orientations get imaged, a procedure much superior to a simple knife edge test. For a simple comparison we will, however, use knife edge test results to quote a single number for the spatial resolution and the performance of the two configurations.

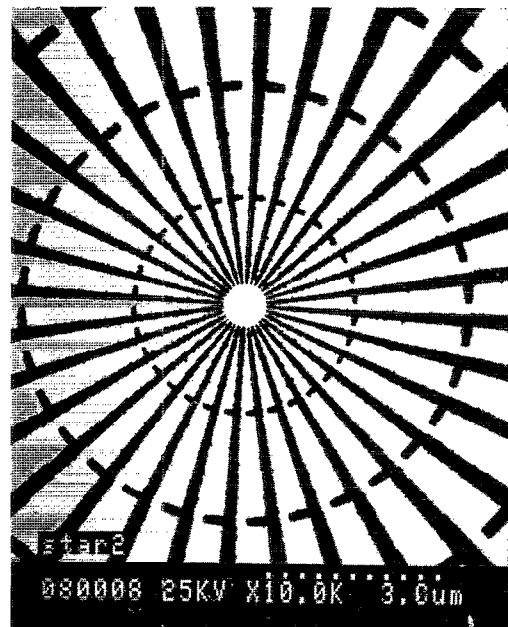


FIG. 1. SEM micrograph of starlike test pattern. Its 32 spokes consist of 100 nm of Au, electroplated on a  $\text{Si}_3\text{N}_4$  membrane. The radial markers have a 2- $\mu\text{m}$  spacing. Hence, the repeat frequency of the spokes at the innermost marker corresponds to about  $2.5 \mu\text{m}^{-1}$ , or a nominal feature size of about 0.2  $\mu\text{m}$ . Note that the mark space ratio is not 1:1, which does not, however, affect the demonstration of the astigmatism correction with elliptical zone plates.

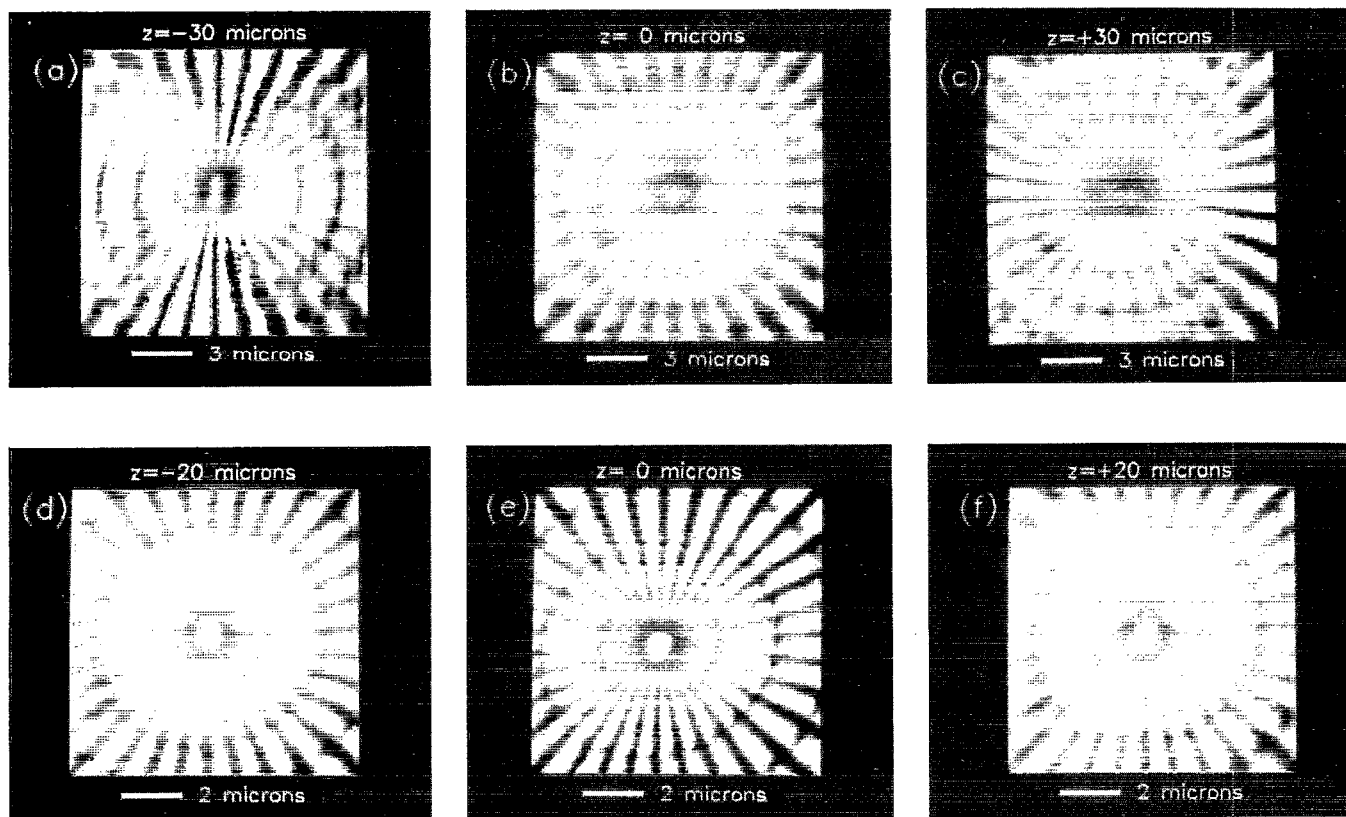


FIG. 2. Transmission x-ray images of the star test pattern for various conditions. Images (a)–(c) were acquired with the round zone plate, with image (b) being in the plane of least confusion, and image (a) and (c) close to the primary and secondary focal planes, respectively. We note that all three images exhibit contrast reversal for certain spatial frequencies and orientations, i.e., the optical transfer function has a zero crossing. The central bright spot has furthermore degenerated into two spots in the primary and secondary focal plane, and the radius markers appears to be split into two lines at various places in all three images. All of these features are artifacts which disappear with the use of the elliptical zone plate, as shown in images (d)–(f). Image (e) is in focus and image (d) and (f) are out of focus by about  $\pm 20 \mu\text{m}$ , respectively. These images, as well as images closer to and more out of focus not shown here, did not reveal any detectable astigmatism. The resolution in image (e) is slightly better in the horizontal (120 nm) than in the vertical (150 nm). Note that the magnification of the top three images is 1.5 times smaller.

The top three micrographs of Fig. 2 show the test pattern imaged with the round zone plate in the plane of least confusion and the primary and secondary focal planes, respectively. We note that even in the plane of least confusion [Fig. 2(b)] contrast reversal for certain spatial frequencies and orientations occurs, which can be easily seen by following spokes from the outside towards the center. In contrast to this, the bottom of Fig. 2 shows three images acquired with an elliptical zone plate, in focus and out of focus by  $\pm 20 \mu\text{m}$ , respectively. Due to eliminated astigmatism and small coma aberrations (see below), these images demonstrate significantly improved spatial resolution compared to the ones taken with the round zone plate. Small asymmetries are still present in all these images, which we attribute to uneven zone plate illumination and transmission, as well as residual alignment errors. We furthermore note that the test pattern appears distorted, which is due to nonlinearities and crosstalk of the scanning stage, as well as some drift. This also makes the horizontal and vertical focus appear slightly tilted.

The smallest features visible in image 2(e) correspond to 120 nm in the horizontal and 150 nm in the vertical. Due to insufficient monochromatization and collimation of the x-ray beam, chromatic aberrations as well as source

size limitations are present, and the Rayleigh resolution  $\delta_R \approx 65 \text{ nm}$  of the zone plate could not be achieved. In the following, we estimate the expected performance and compare it to our results by estimating the various contributions, including the aberrations of the elliptical zone plate itself.

Since an elliptical zone plate as described above is identical to a tilted round zone plate, the aberrations and optical properties of an elliptical plate used on-axis are the same as the off-axis ones of a round zone plate. Field curvature is not important, because we basically image a single point, while spherical aberrations do not depend on the tilt or ellipticity and are negligibly small. Hence, we are left with coma and astigmatism of the third-order Seidel aberrations. Their (relative) size in the plane of least confusion for an object at infinity is<sup>9</sup>

$$\text{coma:astigmatism} = \frac{r_N^2 x'_0}{2f^2} : \frac{r_N x'_0^2}{2f^2} = r_N : x'_0, \quad (1)$$

where  $r_N$  is the radius of the outermost zone,  $f$  is the focal length, and  $x'_0$  is the image distance from the optical axis. Hence, for image points more than a zone plate radius off-axis, astigmatism is dominant. For our purposes, we

have made use of the following corollary: if the astigmatism of an on-axis system, caused by upstream optics, is larger than the astigmatism corresponding to more than a zone plate radius away from the optical axis when caused by a tilted or elliptical zone plate then an elliptical zone plate can reduce the total aberrations, since the increase in coma will be smaller than the original astigmatism. In our case, the astigmatism at 1.86 nm with the round zone plate corresponds to an image distance off-axis of about 7 times the zone plate radius (or a tilt of  $6.3^\circ$ ). The resolution in the plane of least confusion as measured by the 25%–75% intensity rise across an edge was determined to be about  $0.4 \mu\text{m}$ , in agreement with  $0.41 \mu\text{m}$  estimated from Eq. (1). This is 6.3 times the diffraction limit.<sup>10</sup> Hence, the substantial gains in spatial resolution we observed with the use of the elliptical zone plate are consistent with theoretical estimates. The coma aberration introduced with the elliptical zone plate is estimated to be 60 nm, slightly smaller than the diffraction limit.

Resolution limitations arising from insufficient coherent illumination (temporal and spatial) are estimated as follows. The resolving power of the monochromator for the slit sizes used was  $\lambda/\Delta\lambda = 350$ , while for a zone plate with 585 zones it is estimated that  $\lambda/\Delta\lambda \approx 760$  is required for chromatic aberrations to be smaller than the diffraction limit. Hence, chromatic aberrations are present with  $\delta_{\text{chr}} \approx 100 \text{ nm}$ .<sup>11</sup> In the horizontal, the exit slit of the monochromator provides a well-defined source. A slit of  $80 \mu\text{m}$ , used for high flux and short data acquisition times, is, however, too large for diffraction limited imaging and  $\delta_{\text{source}}^h = 62 \text{ nm}$ . Adding the contributions in quadrature (including coma) we arrive at a horizontal resolution of  $\delta^h = 135 \text{ nm}$ , in agreement with the value from the micrographs. In the vertical, the source size is not very well defined. The vertical refocusing configuration was chosen such that, for perfect transport optics, all of the coherent part of the undulator is accepted by the zone plate. However, figure errors of an inexpensive optical element of the beamline, the vertical refocusing mirror, are known to broaden the image of the undulator to an extent consistent with the resolution measured here. Since higher resolution zone plates fabricated by the same process perform in excellent agreement with theory,<sup>12</sup> we expect that with proper collimation (or better refocusing optics) and higher monochromatization the elliptical zone plate would achieve near diffraction limited resolution, as the coma aberrations would contribute only about 60 nm to the spatial resolution.

We have shown that the use of an elliptical zone plate can eliminate astigmatism and significantly improve the spatial resolution of a soft x-ray optical system. The potential gain is larger the more severe the initial astigmatism

[Eq. (1)]. In the case of the X1-SPEM, the spatial resolution improved from about 400 to a source-size limit of 150 nm in the vertical and to 120 nm in the horizontal (chromatic aberration dominated). This successful incorporation of an elliptical zone plate enables the X1-SPEM to further improve the spatial resolution in photoelectron spectromicroscopy, which is now approaching 100 nm.

We would like to thank D. Attwood and D. Kern for their support in zone-plate fabrication, and J. Kirz for reading the manuscript, and making helpful suggestions. This work is in part supported by the National Science Foundation under Grant No. DMR-8815043. The Center for x-ray Optics is supported by the DOE under Contract No. DE-AC-03-76SF00098.

<sup>1</sup> *X-ray Microscopy*, Springer Series in Optical Sciences Vol. 43, edited by G. Schmahl and D. Rudolph (Springer, Berlin, 1984); *X-ray Microscopy II*, Springer Series in Optical Sciences Vol. 56, edited by D. Sayre, M. Howells, J. Kirz, and H. Rarback (Springer, Berlin, 1988); and *X-ray Microscopy III*, Springer Series in Optical Sciences, edited by A. Michette, G. Morrison, C. Buckley (Springer, Berlin, 1992).

<sup>2</sup> For a recent review in zone plate fabrication see E. H. Anderson, *SPIE* **1160** (1989). For earlier work see D. C. Shaver, D. C. Flanders, N. M. Ceglie, and N. I. Smith, *J. Vac. Sci. Technol.* **16**, 1626 (1979).

<sup>3</sup> H. Rarback, Ph.D. dissertation, SUNY at Stony Brook, Stony Brook, 1983.

<sup>4</sup> See for example Y. Vladimirov, D. Kern, T. H. Chang, A. Attwood, H. Ade, J. Kirz, I. McNulty, H. Rarback, and D. Shu, *J. Vac. Sci. Technol.* **B 6**, 311 (1988).

<sup>5</sup> V. Bögli, P. Unger, H. Beneking, B. Greinke, P. Guttman, B. Niemann, D. Rudolph, and G. Schmahl, in *X-ray Microscopy II*, Springer Series in Optical Sciences Vol. 56, edited by D. Sayre, M. Howells, J. Kirz, and H. Rarback (Springer, Berlin, 1988), pp. 80–88.

<sup>6</sup> E. H. Anderson, V. Boegli, M. L. Schattensburg, D. Kern, and H. I. Smith, *J. Vac. Sci. Technol.* **B 9**, 3606 (1991).

<sup>7</sup> H. Ade, J. Kirz, S. Hulbert, E. Johnson, E. Anderson and D. Kern, *Appl. Phys. Lett.* **56**, 1841 (1990); H. Ade, Ph.D. dissertation, SUNY at Stony Brook, Stony Brook, New York, 1990; H. Ade, J. Kirz, S. Hulbert, E. Johnson, E. Anderson and D. Kern, *J. Vac. Sci. Technol.* **A 9**, 1902 (1991).

<sup>8</sup> For some recent applications of the X1-SPEM see H. Ade, C. H. Ko, E. Johnson, E. Anderson, accepted for publication *Surface and Interface Analysis*.

<sup>9</sup> K. Kamiya, *Sci. Light* **12**, 35 (1963); and A. G. Michette, *Optical Systems for Soft X-rays* (Plenum, New York, 1986). We follow the notation of Michette, who's treatment, however, contains some typographical errors. Since we do not have to consider field curvature, the astigmatism/field curvature term is reduced to 1/3 of the combined aberrations. Furthermore, for an estimate in the plane of least confusion rather than the primary or secondary focal planes, the astigmatism term is reduced by another factor of 2.

<sup>10</sup> Our previously published results (Ref. 4) have been acquired with a zone plate with an outermost width of 70 nm instead of the 60 nm used here. The difference in performance is small and the numbers quoted here are furthermore selfconsistent and pertain only to the 60 nm zone plate.

<sup>11</sup> This estimate uses a simple geometric construction, calculating the off-axis distance of the shorter wavelength ray halfway between the interceptions of the long and short wavelength ray with the optical axis.

<sup>12</sup> C. Jacobsen, S. Williams, E. Anderson, M. T. Browne, C. J. Buckley, D. Kern, J. Kirz, M. Rivers, and X. Zhang, *Opt. Commun.* **86**, 351 (1991).